Asian Journal of Pharmaceutical Sciences 17 (2022) 120–128

Available online at www.sciencedirect.com

ScienceDirect

journal homepage: www.elsevier.com/locate/AJPS

Original Research Paper

One-pot preparation of nanodispersion with readily available components for localized tumor photothermal and photodynamic therapy

Anpu Yang[a,b,1], *Yanan Sun*[a,b,1], *Bochen Lyu*[a,b,1], *Binlong Chen*[a,b], *Zhipu Fan*[a,b], *Minghui Li*[a,b], *Yao Zhao*[a,b], *Jijun Fu*[c], *Bing He*[a,b], *Hua Zhang*[a,b], *Xueqing Wang*[a,b], *Wenbing Dai*[a,b,*], *Qiang Zhang*[a,b,*]

[a] *State Key Laboratory of Natural and Biomimetic Drugs, School of Pharmaceutical Sciences, xueyuan road 38, haidian district, Peking University, Beijing 100191, China*

[b] *Beijing Key Laboratory of Molecular Pharmaceutics, School of Pharmaceutical Sciences, Peking University, Beijing 100191, China*

[c] *School of Pharmaceutical Science, Guangzhou Medical University, Guangzhou 511436, China*

ARTICLE INFO

Article history:
Received 14 April 2021
Revised 2 August 2021
Accepted 6 September 2021
Available online 31 October 2021

Keywords:
Photodynamic therapy
Photothermal therapy
Carbon nanohorn
Zinc phthalocyanine

ABSTRACT

Photothermal (PTT) and photodynamic (PDT) combined therapy has been hindered to clinical translation, due to the lack of available biomaterials, difficult designs of functions, and complex chemical synthetic or preparation procedures. To actualize a high-efficiency combination therapy for cancer via a feasible approach, three readily available materials are simply associated together in one-pot, namely the single-walled carbon nanohorns (SWCNH), zinc phthalocyanine (ZnPc), and surfactant TPGS. The established nanodispersion is recorded as PCT. The association of SWCNH/ZnPc/TPGS was confirmed by energy dispersive spectrum, Raman spectrum and thermogravimetric analysis. Under lighting, PCT induced a temperature rising up to about 60 °C due to the presence of SWCNH, production a 7-folds of singlet oxygen level elevation because of ZnPc, which destroyed almost all 4T1 tumor cells *in vitro*. The photothermal effect of PCT depended on both laser intensity and nanodispersion concentration in a linear and nonlinear manner, respectively. After a single peritumoral injection in mice and laser treatment, PCT exhibited the highest tumor temperature rise (to 65 °C) among all test groups, completely destroyed primary tumor without obvious toxicity, and inhibited distant site tumor. Generally, this study demonstrated the high potential of PCT nanodispersion in tumor combined therapy.

* Corresponding authors.
E-mail addresses: daiwb@bjmu.edu.cn (W.B. Dai), zqdodo@bjmu.edu.cn (Q. Zhang).

[1] These authors contributed equally to this work.

Peer review under responsibility of Shenyang Pharmaceutical University.

https://doi.org/10.1016/j.ajps.2021.09.003

1. Introduction

Photodynamic therapy (PDT) and photothermal therapy (PTT) are potential anti-tumor strategies in which a photosensitizer/photothermal agent accepts the lighting and produces reactive oxygen species (ROS) or heat and induces cell apoptosis or directly kill cells [1,2]. The advantages of PDT and PTT are reflected in their powerful ability to destruct tumors, their high selectivity to tumor tissue, and their small damage to normal tissue [1,3]. In addition, they have a wide range of anti-tumor activities, and various solid tumors could respond to this treatment [4,5]. There are many studies on designing new systems to achieve better PDT/PTT combination therapy [6–8]. However, in these studies, scarce raw materials, complex chemical synthetic and pharmaceutical preparation methods, and multiple responses designs have hindered clinical translation [1].

Inorganic-organic hybrid materials possess inorganic and organic advantages in terms of stability in inorganic compound and functional in organic compound [9,10]. Single-wall carbon nanohorns (SWCNH) are a kind of inorganic compound with closed cages of sp2-bonded carbon atoms [11]. In our previous work, SWCNH improves biocompatibility over nanotubes by triggering less protein-initiated pyroptosis and apoptosis in macrophages, and it exhibits a wilder application [12]. For instance, SWCNH was found to inhibit the proliferation of hepatoma cells [13], and it was used to load anti-inflammatory dexamethasone for sustained release [14]. Another system applied the BSA conjugated and oxidized SWCNH to achieve PTT therapy after intratumoral injection [15].

Porphyrin-like compounds are the most commonly used organic photosensitizers. Among them, phthalocyanine is efficient in light absorption with a much higher absorption coefficient than porphyrin [1,16]. It exhibits the maximum absorption in the phototherapeutic window and has easier synthetic access than other photosensitizing cores absorbing in the same range of wavelengths (such as bacteriochlorins) [17]. Phthalocyanine can form complexes with H^+ and metal ions, such as Zn^{2+}, Cu^{2+}, Al^{3+} etc., and the photodynamic efficiency of zinc phthalocyanine (ZnPc) is the highest [18]. Some types of phthalocyanines have already entered into the clinical trials, including silicon-substituted phthalocyanine PC422, cationic phthalocyanine RLP068 [19], and Photocyanine (Suftalan Zinc) [20]. Finally, D-α-tocopherol polyethylene glycol 1000 succinate (TPGS), an approved pharmaceutical excipients, is a high-efficiency surfactant which can facilitate and stabilize the dispersion of hydrophobic nano-system in water with low toxicity [21].

In this study, we engineered the nanodispersion of ZnPC/SWCNH/TPGS (PCT) for the first time in one-pot preparation with TPGS acting as a stabilizer. The properties of PCT were characterized. Especially, the serial qualitative and quantitative studies were conducted to confirm the association of ZnPc with SWCNH. We also tested how illumination intensity and nanodispersion concentration affected the photothermal of PCT. Additionally, the photodynamic and photothermal ability of PCT were investigated and their combined therapy on triple negative breast cancer (TNBC) model was studied both *in vitro* and *in vivo*. Finally, we observed the toxicity of PDT/PTT therapy with PCT. In all, this study established a PCT nanosystem with readily available components through One-pot preparation and demonstrated its high potentiality in tumor combined therapy.

2. Materials and methods

2.1. Materials

Zinc phthalocyanine (ZnPc, Strem Chemicals, Inc., American) and single-walled carbon nanohorns (SWCNH, Qingdajiguang Co. Ltd., China) were used as PDT/PTT agent, respectively. D-α-tocopherol polyethylene glycol 1000 succinate (TPGS, Aladdin Co. Ltd., China) were selected as a stabilizer. Dimethyl sulfoxide (DMSO, Sinopharm Chemical Reagent Beijing Co. Ltd., China) and ethanol (Eth, Sinopharm Chemical Reagent Beijing Co. Ltd., China) of analytical grade were added as solvents to promote ZnPc and SWCNH adsorption. Singlet oxygen sensor green reagent (SOSG, Thermo Fisher Co. Ltd., American) was used to detect singlet oxygen concentration after PDT therapy. Cell Counting Kit-8 (CCK-8, Beyotime Biotechnology Co. Ltd., China) was used to investigate cell viability after therapy. Tribromoethanol (Energy Chemical Co. Ltd., China) was used as an anesthetic for mice. Fetal bovine serum (FBS, PAN Biotech Co. Ltd., Germany), dulbecco's modified eagle medium (DMEM, Macgene Co. Ltd., China), penicillin-streptomycin solution (Macgene Co. Ltd., China), and trypsin (Macgene Co. Ltd., China) were used for cell culture.

2.2. Preparation of PCT nanodispersion

Three types of nanodispersion including ZnPc/TPGS (ZPT), SWCNH/TPGS (SCT) and ZnPc/SWCNH/TPGS (PCT) were prepared. PCT was prepared as following: 10 mg ZnPc was added into 25 ml mixed solution of DMSO/ethanol (1:1, v/v). The mixture was sonicated for 1 h using probe sonicator in 80 W with 5 s interval after working for 5 s and then stirred for 24 h before being centrifuged for 5 min at 5000 rpm to obtain the supernatant, which was the saturated solution of ZnPc. Next, 10 mg SWCNH was added into the above supernatant, sonicated for 1 h before being stirred for 48 h to ensure satisfying adsorption of ZnPc on SWCNH. The prepared ZnPc/SWCNH was separated by filtration, washed several times, and dried. PCT nanodispersion was constructed by adding 2 mg ZnPc/SWCNH into 2 ml DMEM containing 10 mg TPGS and sonicating for 1 h. ZPT and SCT were prepared by adding ZnPc or SWCNH instead of ZnPc/SWCNH into DMEM solution of TPGS. The above operations were carried out in the dark.

2.3. Morphology of PCT nanodispersion

Particle size and morphology of PCT were characterized by dynamic light scattering (DLS) analysis using a Malvern Zetasizer Nano ZS and JEOL JEM-2100F high resolution transmission electron microscope (TEM).

2.4. Verification the binding between ZNPC and SWCNH

Zn, O, C elements analysis were carried out by energy dispersive spectrum (EDS) using JEM-2100F high resolution transmission electron microscope. Fluorescence spectrums of SCT, ZPT and PCT were characterized with the excitation and emission spectrum in the range of 580–630 nm and 650–730 nm separately with F-7000 fluorescence spectrum. Raman spectrum and FT-Infrared spectrum of ZnPc, SWCNH and ZnPc/SWCNH were obtained, as well as thermogravimetric analysis (TGA) ranging from 25 to 900 °C at a rate of 10 °C/min.

The ZnPc release behavior was evaluated using the dialysis method. We first measured the standard curve of ZnPc in PBS (1% Tw80) using UV–VIS absorption spectrometry. The release mediums were pH 7.4 PBS solution, to improve the water solubility of ZnPc, 1% Tween 80 (v/v) was added to the release medium. The drug release curves were measured in a gas bath thermostatic oscillator with a shaken speed of 100 rpm at 37 °C. Each 1 ml sample was taken out from the different release mediums, and with the addition of the same fresh medium.

2.5. Photothermal efficacy in vitro

TPGS, SCT, ZPT and PCT (1 ml) were placed in 24-well plate and, they were exposed to 660 nm laser for 10 min. Temperatures at different time points were recorded by thermal infrared camera to draw temperature-time curves. The above solution or nanodispersion with the concentration of SWCNH and/or ZnPc fixing at 117.28 and 32.72 μg/ml were exposed to laser (660 nm, 300 mW/cm^2). Meanwhile, PCT (300 μg/ml) was exposed to 660 nm laser with varied intensity: 100, 150, 200, 300 mW/cm^2. At the same time, PCT with different concentrations of 0, 10, 20, 50, 100, 150, 200, 300 μg/ml were exposed to laser (660 nm, 300 mW/cm^2).

2.6. Photodynamic efficacy in vitro

SOSG was added into SCT, ZPT and PCT to make the final concentration of 10 μg/ml, and the ex/em fluorescence intensity of the nanodispersion was measured under 504/525 nm. After being exposed to 660 nm laser at 2 W/cm^2 for 5 min, the nanodispersion was centrifugated at 14 000 rpm for 10 min and, the fluorescence intensity of the supernatant was measured. The difference in value reflects the photodynamic efficacy.

2.7. Cytotoxicity and ROS studies

4T1 cells were seeded in a 96-well plate at a density of 5000 cells/well. After incubation at 37 °C for 24 h, SCT, ZPT and PCT were added separately at the final concentration of SWCNH and/or ZnPc was 7.82 and 2.18 μg/ml. After further incubation at 37 °C for 24 h, each well was exposed to laser (660 nm, 800 mW/cm^2) for 5 min. The plate was further incubated for 3 h, then the culture medium was discarded, and the wells were washed by PBS twice. Cell viability was measured by CCK-8 method. Cells treated with fresh culture medium and exposed to 660 nm laser were used as the control group.

4T1 cells were seeded in a glass-bottom confocal plates with 5×10^4 cells per well. Then, the cells were incubated with PCT over night. Next, the plate was irradiated with a pulsed near-infrared laser (800 mW/cm^2, 5 min) at 660 nm and incubated overnight. The cells were washed with PBS 3 times and stained with Calcein-AM/PI buffer for 30 min.

Intracellular ROS was detected by using DCFH-DA reactive oxygen species assay kit. 4T1 cells were seeded in 24-well plate with 1×10^5 cells per well and incubated overnight. Then, the cells were incubated with SCT, ZPT and PCT at 37 °C for 4 h. Next, the cells were cultured with DCFH-DA at 37 °C for 20 min, washed 3 times with PBS, and irradiated with a pulsed near-infrared laser (800 mW/cm^2, 5 min) at 660 nm. The DCF fluorescence images were immediately detected by a fluorescence microscope (Olympus).

2.8. Peritumoral treatment in tumor-bearing mice model

The breast cancer model was established by subcutaneous inoculation of 1×10^6 4T1 cells in the right thigh of 5-week old Balb/c mice. The mice were randomly divided into six groups with five mice in each group: PBS, PCT, PBS with laser (PBS + L), SCT with laser (SCT + L), ZPT with laser (ZPT+L), PCT with laser (PCT+L). When the tumor volume reached approximately 60 mm^3, the mice were peritumoral treated with drugs. In detail, 100 μl of PBS, SCT, ZPT or PCT with the concentrations of SWCNH and/or ZnPc fixing at 7.82 mg/kg and 2.18 mg/kg, respectively, was peritumoral injected. Because we got satisfactory results with a single treatment, we didn't give multiple doses of PCT or multiple irradiations. Based on our previous study, the PCT distributed in the tumor at a high level 24 h after injection, so these tumors were exposed to laser at 24 h after peritumoral treatment. 24 h later, tumor area of the later four groups were exposed to laser (660 nm, 2 W/cm^2) for 5 min. Temperatures at different times were recorded by thermal infrared camera. Tumor volumes of the animals were recorded every other day and calculated according to the following formula: $V = 1/2 \times \text{length} \times \text{width}^2$. On Day 19 after implantation, mice were sacrificed, and the tumors were excised and weighed.

2.9. Photodynamic efficacy in vivo

The 4T1 tumor model was established by subcutaneous inoculation of 3×10^5 4T1 cells in the right hind leg of female BALB/c mice. When the tumor volume reached approximately 250 mm3, the mice were randomly divided into four groups: SCT+NIR, ZPT+NIR, PCT and PCT+NIR. The mice were peritumoral treated with 100 μl of SCT, ZPT or PCT with the concentrations of SWCNH and/or ZnPc fixing at 7.82 mg/kg and 2.18 mg/kg, respectively. After 24 h, the mice were intratumorally injected with DCFH-DA at a dose of 2.5 mg/kg. Ten minutes later, tumor areas of the SCT, ZPT and PCT groups were exposed to laser (660 nm, 2 W/cm^2) for 5 min. Then, the tumors were collected and frozen with OTC embedding medium at frozen section of 10 μm thickness, stained with DAPI, then observed by using Polaris Multispectral Tissue Imaging Quantitative Analysis System.

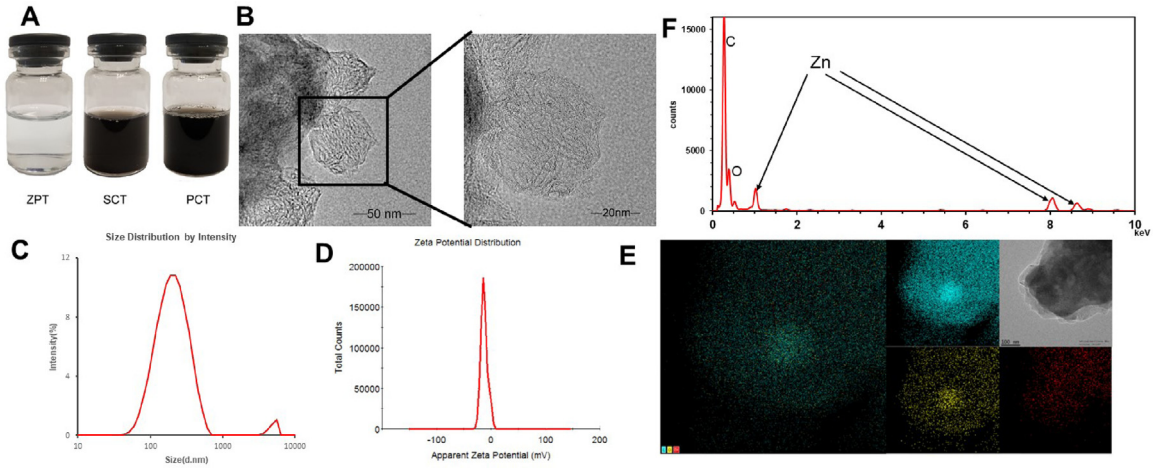

Fig. 1 – (A) Picture of ZPT, SCT and PCT nanodispersion, SWCNH: 39.09 μg/ml and ZnPc: 10.91 μg/ml . (B) TEM image of PCT nanodispersion. (C) Size distribution of PCT by DLS. (D) Zeta potential distribution of PCT. (E) STEM image of PCT with element C (blue), O (yellow), Zn (red) and their mapping image. (F) EDS of PCT. (For interpretation of the references to colour in this figure legend, the reader is referred to the web version of this article).

2.10. *Biocompatibility evaluation and abscopal effect*

The breast cancer model was established by subcutaneous inoculation of 1×10^5 4T1 cells in both the left and right thigh of Balb/c mice. The mice were randomly divided into 3 groupswith five mice in each group: PBS, PCT and PCT+L. After treatment, tumor volumes of the animals were calculated and recorded every other day. On Day 19 after implantation, mice were sacrificed, and the tumors and major organs including heart, liver, spleen, kidney, and lung were excised. The excised organs were fixed in 10% neutral formalin, and then sliced and H&E stained.

3. Results and discussion

3.1. *Preparation of PCT nanodispersion and their preliminary characterization*

Three types of aqueous nanodispersion were prepared including ZPT, SCT and PCT. The concentrations of SWCNH and ZnPc were measured to be 39.09 and 10.91 μg/ml in PCT nanodispersion, and those in ZPT or SCT were comparable to these numbers. Here, TPGS was favorable for the dispersion of three kinds' nanodispersion into PBS. It was supposed that the hydrophobic and sp2 hybridized π bonds in the structures of both ZnPc and SWCNH facilitated the association of these two functional nanomaterials through physical adsorption [16,22,23].

Among the three nanodispersion, ZPT presented a nattier blue color, while SCT and PCT showed deep black due to the presence of SWCNH (Fig. 1A). The TEM image of PCT nanodispersionexhibited a dahlia-like structure (Fig. 1B), which was consistent with the previous report on SWCNH in an aqueous medium [16]. The structure of PCT shown in Graphical Abstract is somehow different from its TEM image in Fig. 1B, likely due to the fact that only SWCNH can be visualized under the TEM. The scale of PCT in TEM was about 50 nm. Then, it was found that the size evaluated by DLS was more than 100 nm (Fig. 1C) and the zeta potential of PCT nanodispersionwas −12.6 mV (Fig. 1D). There are some factors that might lead to the difference in size measurement. For instance, the dynamic process in DLS determination or the sample preparing procedure in TEM study. On the other hand, ZnPc crystals were not observed under TEM. To confirm the existence of ZnPc, a scanning transmission electron microscope (STEM) was adopted. In the mapping image of three main elements, C, O and Zn co-localized well with each other as shown in Fig. 1E, indicating the formation of PCT. The bright round area in the central part of C and O images was owing to the carbonization during STEM study.

3.2. *Components and spectroscopy study of PCT nanodispersion*

Firstly, EDS under 0–10 keV demonstrated the existence of C, O and Zn elements again, and simultaneously it was found that the percentage of Zn atom was 0.91% among all atoms of the selected field (Fig. 1F). As shown in Fig. 2A and 2B, PCT had a peak in 610 nm and 685 nm in excitation and emission fluorescence spectrum, respectively, which accorded with the related fluorescence spectrum of ZPT. But SCT did not exhibit any peaks in such spectroscopy study. On the other hand, the absorption spectrum of PCT showed a peak at 700 nm (Fig. 2C). To verify its source, TPGS and ZnPc's absorption spectra were scanned. It was found in Fig. 2D that TPGS almost had no peak in 450–1000 nm, but ZnPc presented a strong absorption peak around 700 nm, so it was inferred that the peak in 700 nm resulted from ZnPc. Next, the Micro-Raman imaging spectrometer was conducted to confirm the reduced lattice imperfection of carbon nanohorn in the presence of ZnPc in the PCT nanodispersion, because of hydrophobic and π-π conjugation effect between SWCNH and ZnPc. It was clear then that, compared with SCT, the I_D:I_G of PCT

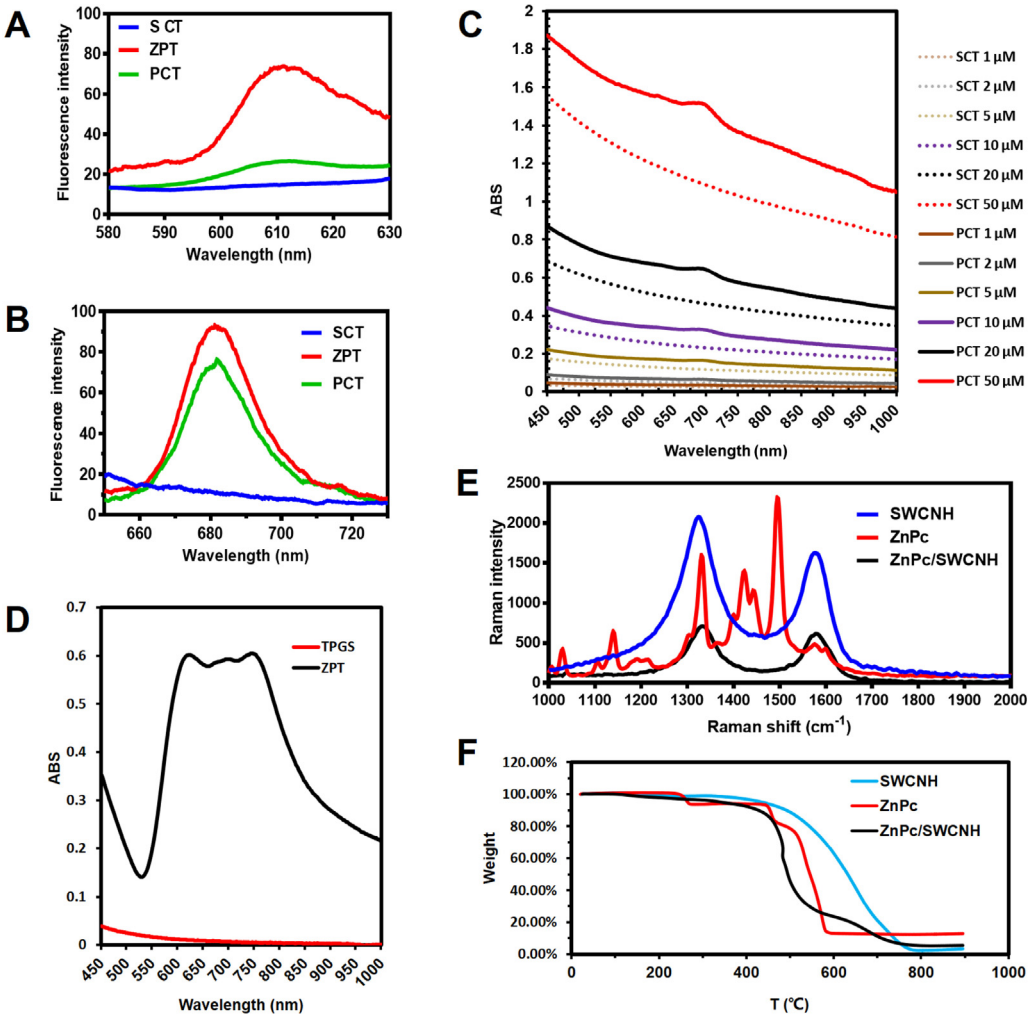

Fig. 2 – Excitation (A) and emission (B) spectrum of SCT, ZPT and PCT. (C) Absorption spectrum of SCT and PCT in different concentration. (D) Absorption spectrum of TPGS and ZPT. (E) Raman spectrum of SWCNH, ZnPc and ZnPc/SWCNH. (F) TGA curve of SWCNH (blue line), ZnPc (red line) and ZnPc/SWCNH (black line) in air. (For interpretation of the references to colour in this figure legend, the reader is referred to the web version of this article).

had a descend from 1.273 to 1.154 (Fig. 2E), which actually demonstrated the reduced lattice imperfection of PCT. Finally, the FTIR spectrometry revealed that there were some similar peaks between ZnPc and ZnPc/SWCNH (Fig. S1). Generally, based on the serial studies in EDS, fluorescence excitation and emission spectrum, ultraviolet-visible absorption spectrum, Raman spectrum and FITR spectrum, it was confirmed that ZnPc did associate with ZnPc/SWCNH and PCT. The drug release profile of ZnPc in pH 7.4 PBS (1% Tw80 and 3% Tw80) might also confirm the adsorption of ZnPC on the single-walled carbon nanohorns (Fig. S2).

Additionally, the amount of ZnPc in nanodispersion was also very important, since it might decide the efficacy of photodynamic and photothermal therapy. Here, thermogravimetric analysis (TGA) method was applied to measure the percentage of ZnPc in ZnPc/SWCNH. With a rising rate of 10 °C/min in air, TGA study could obtain the weight loss of every test component. In this experiment, the loss of ZnPc, SWCNH and ZnPc/SWCNH was 86.978%, 95.8% and 94.02%, respectively (Fig. 2F). According to the following formula established through quality loss among three analytes,

$$SWCNH\% = [loss(ZnPc/SWCNH) - loss(ZnPc)]/[loss(SWCNH) - loss(ZnPc)] \times 100 ZnPc\% = 1 - SWCNH\% \quad (24)$$

There was 20.18% ZnPc and 79.82% SWCNH in the ZnPc/SWCNH. In N_2 atmosphere, pure ZnPc lost 71.94% weight, SWCNH had hardly loss, and ZnPc/SWCNH lost 16.86% (Fig. S3), so there was 23.44% ZnPc and 76.56% SWCNH in the ZnPc/SWCNH according to the formula. Averaging the results in N_2 and air, there was 21.81% ZnPc and 78.19% SWCNH in the ZnPc/SWCNH. On the other hand, we could calculate the percent of ZnPc in PCT via quantifying the TPGS that we added in the ZnPc/SWCNH, which was 3.64% of PCT. As mentioned above, the percentage of Zn atom was 0.91% in all atoms of the selected field in PCT (Fig. 1D).

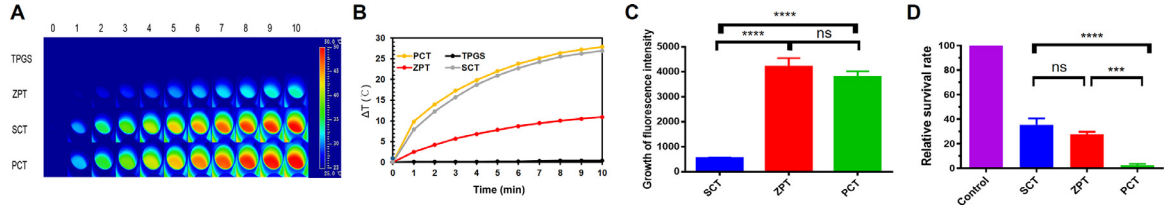

Fig. 3 – (A) Comparison of temperature rise among four test materials (TPGS, ZPT, SCT and PCT) under 300 mW/cm^2 660 nm laser at different times. (B) The corresponding temperature-time curves of the four test materials under 300 mW/cm^2 660 nm laser. (C) Comparison of singlet oxygen production efficiency among SCT, ZPT and PCT evaluated by Singlet Oxygen Sensor Green reagent (SOSG). (D) Survival rate of 4T1 cells after administration of SCT, ZPT or PCT and 800 mW/cm^2 660 nm laser for 5 min. Statistical analysis is based on the two-tailed, unequal variance Student's *t*-test (error bars, s.e.m.), ***P < 0.001, ****P<0.0001.

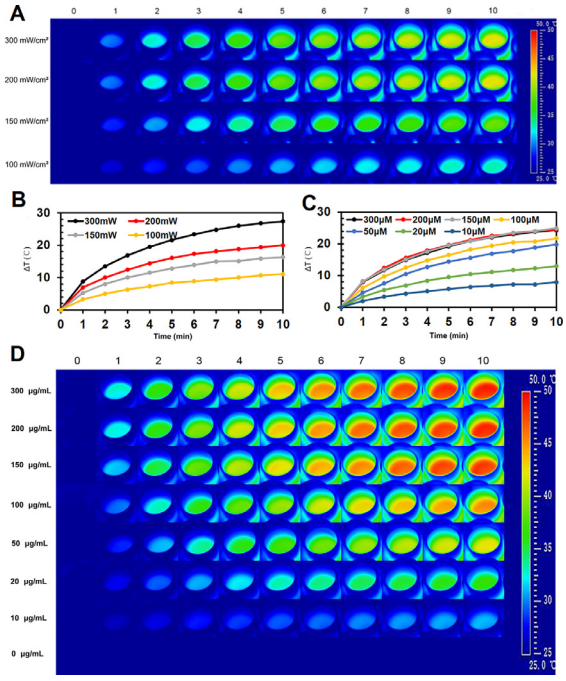

Fig. 4 – (A) Temperature rise images of PCT over time under different laser intensity from 100, 150, 200 to 300 mW/cm^2 by thermal infrared camera. (B) The corresponding temperature-time curves of PCT under different laser intensity. (C) The temperature-time curves of PCT under different PCT concentration. (D) Temperature rise images of PCT over time under different PCT levels from 0, 10, 20, 50, 100, 150, 200 to 300 μg/ml.

3.3. *Photodynamic and photothermal ability of PCT nanodispersion in vitro*

PTT is based on temperature control in tumor tissue. Here, temperature rises of TPGS, SCT, ZPT and PCT after different exposure time to laser were investigated first *in vitro*. As directly shown in Fig. 3A, the color of some test materials changed clearly from shallow to deep, suggesting the temperature rise of some aqueous nanodispersion in the test situation. Quantificationally, PCT's temperature raised 27.9 °C under 300 mW/cm^2 660 nm laser for 10 min. Under the same condition, the temperature of SCT went up 26.9 °C, and that of ZPT ascended only 10.9 °C, while TPGS hardly had a temperature rise (Fig. 3B). This phenomenon distinctly revealed that the SWCNH contributed most to photothermal efficiency, followed by the weak effect of ZnPc, and the almost no effect of TPGS.

PDT mainly depends on the singlet oxygen newly produced under lighting. Here, the SOSG was utilized to measure the singlet oxygen level in order to evaluate the photodynamic efficacy. Fig. 3C presents the growth of fluorescence intensity which indicates the level of singlet oxygen of test materials after exposure to the laser. It was found that the singlet oxygen level of PCT and ZPT was 7-folds that of SCT. In other words, the photodynamic efficiency of test samples majorly came from ZnPc, rather than SWCNH or TPGS. There was no significant difference between the PCT and ZPT groups in singlet oxygen levels. The SOSG test showed that, with the increase of concentration and intensity, the capacity of PCT in singlet oxygen production was enhanced (Fig. S4 and S5).

The photodynamic and photothermal effect of PCT on tumor cells *in vitro* was investigated, 4T1 cells were used in this study. The 4T1 breast cancer is a transplantable tumor cell line that is highly tumorigenic and invasive. It is a frequently used experimental animal model for triple negative breast cancer. We first evaluated the IC50 of SCT, ZPT or PCT on 4T1 cells (Fig. S6). The survival rate of 4T1 cells after treatment with SCT, ZPT or PCT together with 800 mW/cm^2 660 nm laser for 5 min is given in Fig. 3D. It was noticed that, after lighting, SCT and ZPT treatment resulted in 35% and 28% cell survival, respectively. Here, as the control treatment, ZPT actually indicated the *in vitro* photodynamic effect, while SCT group represented mostly the photothermal one. Finally, the cell survival rate in the PCT group was only 2.4%, namely, almost all test cells were killed. The significantly high efficiency of PCT than other control groups *in vitro* revealed that combined photodynamic and photothermal therapy was more efficient than each of the two strategies.

The Calcein-AM/PI double assay was consistent with the cytotoxic evaluation (Fig. S8). We also evaluated the photodynamic effect on tumor cells. The DCFH-DA was used for detecting the ROS generation in 4T1 cells treated with SCT, ZPT or PCT. All three groups showed almost no signals without laser irradiation. When irradiated with NIR laser, the ZPT and PCT groups showed a DCFH signal, indicating the generation of ROS (Fig. S9).

3.4. *Impact of illumination intensity and concentration on photothermal of PCT nanodispersion*

Here, PTT was further investigated in terms of its action law under different laser illumination intensities or different concentrations of PCT. In the range of 100 mW/cm^2 to 300 mW/cm^2 laser lighting, the temperature rise was found to be proportional to the laser illumination intensity during 0 min-10 min for 300 μg/ml of PCT (Fig. 4A and 4B). However, there seemed a "ceiling effect" for the impact of PCT concentration. In other words, in a lower concentration of PCT like 10–50 μg/ml, there was a liner relationship between temperature and concentration under 300 mW/cm^2 laser for 10 min. But as concentration increased beyond 1500 μg/ml, no more rise in temperature was noticed. For instance, the curves of temperature rise in 150, 200 and 300 μg/ml groups almost completely overlapped, and all of them approached 25 °C (Fig. 4C and 4D).

3.5. *Photodynamic and photothermal therapy of PCT nanodispersion after local administration*

Firstly, a 4T1 tumor-bearing Balb/c mouse model was established by subcutaneous inoculation of cancer cells in the right thigh of mice. Then, the right tumor was taken as the test side. PBS, SCT, ZPT or PCT nanodispersion was administered to the tissue around the right tumor, and a 660 nm laser was adopted to light the right tumor, followed by the record of tumor temperature, tumor volume and weight (Fig. 5A). As seen in Fig. 5B and C, the temperature rises of tumors from high to low had a sequence of PCT > SCT > ZPT > PBS. Before laser treatment, the body temperature of test mice was 35.2–37.1 °C, and after lighting, the local temperature of PCT, SCT, ZPT and PBS group increased to 65.2 °C, 54.4 °C, 47.7 °C and 39.6 °C, respectively. Namely, the PCT exhibited the highest temperature rise, and the *in vivo* test was in good accordance with the *in vitro* study.

In terms of tumor size, it was observed that the tumors in control (PBS) group grew very fast (Fig. 5D), and at the end of test (Day 19) it was about 10-fold of the initial size. In SCT group, although two tumors disappeared (Fig. 5E), others reached ~350 mm^2, which was about 6-folds of the initial size and confirmed the photothermal effect in certain content. In the ZPT group, the tumors grew to only 100 mm^2 in 19 d Although the average values with the variance of relative survival rate in ZPT group were lower than the SCT group, there was no significance between these two groups statistically, which was consistent with the cytotoxicity study. Importantly, it was surprising to find that tumors of the PCT group at the same test condition disappeared with only charred spots remained, which proved that the combined photodynamic and photothermal therapy was a very efficient approach to wipe out tumor.

Compared with another type of control, namely the PCT group without laser, the PCT group with laser exhibited significantly better efficacy, suggesting the key role of lighting in this strategy. The PCT group without laser showed slightly better therapy than the PBS group, likely due to the TPGS used in the PCT system, since high concentration surfactant was found to be cytotoxic to tumor (Fig. S7). As shown in Fig. S10, the DCFH green fluorescence distributed nearly throughout the tumor section of the PCT group with laser irradiation, indicating the generation of ROS. As shown in Fig. 5F, the therapy effect based on tumor weight at the end of test had a sequence from high to low: PCT+*L* > ZPT+*L* > SCT+*L* > PBS+*L*. It was different from the sequence of temperature rise mentioned above, because of the photodynamic effect.

3.6. *Abscopal effect of PCT based photodynamic and photothermal therapy*

Some studies found that there was an "abscopal effect" during photodynamic and photothermal therapy. This type of treatment had some impact on the control tumors without treatment (or with only PBS) [23]. Here, the abscopal effect was also investigated. Firstly, a similar mouse tumor model was established with the right tumor as the test side and the left tumor as the control side (Fig. 6A). After PCT was administered to the tissue around the right tumor and the laser was exposed to the right tumor, the tumor sizes on the left side were recorded (Fig. 6B and 6C). The left tumor volume in the PCT group was smaller than that of the PBS group, namely, the combined photodynamic and photothermal therapy here did impact the untreated tumors, which confirmed the so-called abscopal effect in such situation. It was supposed that the immune system might play a key role here [24–26].

3.7. *Preliminary toxicity of PCT based photodynamic and photothermal therapy*

The potential *in vivo* toxicity is always a crucial issue for a nanomedicine system. Firstly, the H&E staining sections of main organs, heart, liver, spleen, lung and kidney after local administration of PBS, PCT and PCT with laser treatment are presented in Fig. 6D. It was clear that there was no significant difference among these test groups. Secondly, the body weights of mice after the photodynamic and photothermal therapy are illustrated in Fig. S11. Briefly, there was no significant change of the body weights for all test groups compared to the PBS group. Thus, this revealed that no obvious toxicity was found for all nanodispersion systems investigated under the study conditions.

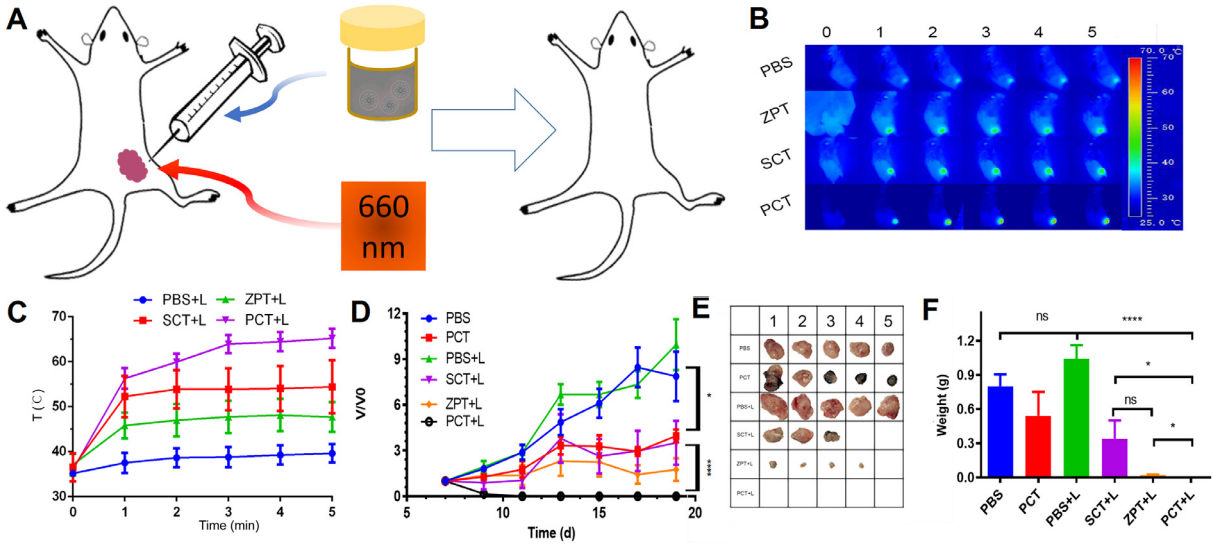

Fig. 5 – Photodynamic and photothermal therapy *in vivo* ($n = 5$). (A) Schematic diagram of photodynamic and photothermal therapy in 4T1 bearing BALB/c mice (2 W/cm^2, 660 nm) ($n = 5$). (B) *In vivo* photothermal temperature curves of the tumor region with different groups and (C) its corresponding temperature growth curves. (D) Tumor volume growth curves for different treatments. (E) The tumor images after mice were executed at the 20th day (1 cm^2 per box). (F) The tumor weights from different treatments at the end of efficacy test. Statistical analysis is based on two-tailed, unequal variance Student's *t*-test (error bars, s.e.m.), *$P < 0.05$, ****$P < 0.0001$.

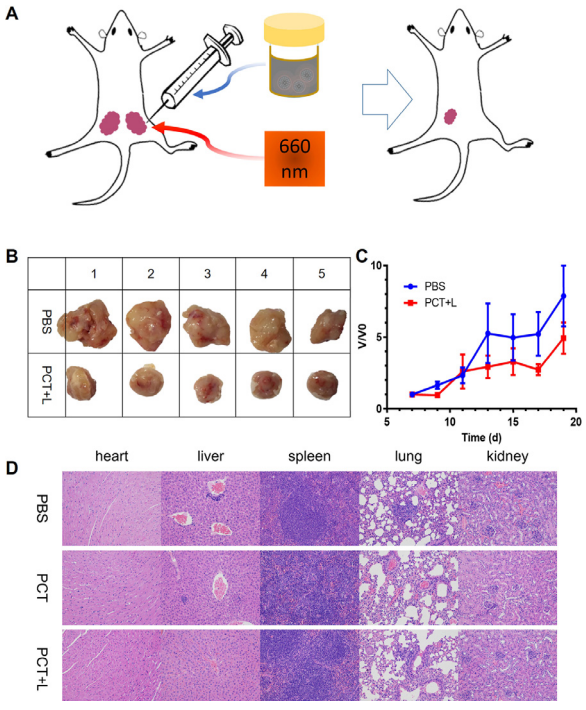

Fig. 6 – Abscopal effect and organ toxicity in PCT based therapy ($n = 5$). (A) The model that Balb/c mice bearing two 4T1 tumors on right and left haunches, respectively. Administration of PCT around the right tumor and lighting with 2 W/cm^2 660 nm laser to right tumor (PCT+L). (B)The left tumor's picture at Day 20 and (C) the relative volume curve. (D) Histologic section of main organs with H&E stain.

4. Conclusion

In the present study, a nanodispersion system of ZnPC/SWCNH/TPGS (PCT) was engineered in a one-step way and investigated *in vitro* and *in vivo* for the first time. Simultaneously, comparing with its controls of ZnPc/TPGS (ZPT) and SWCNH/TPGS (SCT) systems, in terms of physicochemical features, photodynamic and photothermal ability, therapeutic outcome, and toxicity in the TNBC model. Other studies were also conducted to identify the association of ZnPc with SWCNH, the effect of illumination intensity and nanodispersion concentration on PDT and PTT, the impact of different delivery route, and the influence of PDT/PTT treatments on the untreated or control tumor.

Before dispersing into TGPS solution, ZnPC and SWCNH readily associated together taking the advantage of the hydrophobic and π-π conjugation effect between them, which was confirmed by a series of qualitative and quantitative studies such as EDS, Raman spectrum and thermogravimetric analysis. It was found that the PCT nanosystem could induce the highest temperature rise and strongest antitumor efficacy under lighting among test groups *in vitro* and *in vivo*, with no significant toxicity. After treatment, tumors in PCT group even disappeared. In combined therapy, and the photodynamic and photothermal ability mostly came from ZnPC and SWCNH, respectively. The photothermy of PCT depended on laser intensity and PCT concentration. Briefly, it was demonstrated that PCT nanodispersion was a potential candidate in further antitumor combination therapy.

Conflicts of interest

The authors report no conflicts of interest. The authors alone are responsible for the content and writing of this article.

Acknowledgements

The work was supported by the National Natural Science Foundation of China (81690264), the National Basic Research Program of China (2015CB932100) and the Innovation Team of the Ministry of Education (BMU20110263).

Supplementary materials

Supplementary material associated with this article can be found, in the online version, at doi:10.1016/j.ajps.2021.09.003.

REFERENCES

[1] Li X, Lovell JF, Yoon J, Chen X. Clinical development and potential of photothermal and photodynamic therapies for cancer. Nat Rev Clin Oncol 2020;17(11):657–74.
[2] Deng X, Shao Z, Zhao Y. Solutions to the drawbacks of photothermal and photodynamic cancer therapy. Adv Sci (Weinh) 2021;8(3):2002504.
[3] You Q, Sun Q, Wang J, Tan X, Pang X, Liu L, et al. A single-light triggered and dual-imaging guided multifunctional platform for combined photothermal and photodynamic therapy based on TD-controlled and ICG-loaded CuS@mSiO(2). Nanoscale 2017;9(11):3784–96.
[4] Allison RR, Sibata CH, Downie GH, Cuenca RE. A clinical review of PDT for cutaneous malignancies. Photodiagnosis Photodyn Ther 2006;3(4):214–26.
[5] Casas A, Di Venosa G, Hasan T, Al B. Mechanisms of resistance to photodynamic therapy. Curr Med Chem 2011;18(16):2486–515.
[6] Liu Y, Zhi X, Yang M, Zhang J, Lin L, Zhao X, et al. Tumor-triggered drug release from calcium carbonate-encapsulated gold nanostars for near-infrared photodynamic/photothermal combination antitumor therapy. Theranostics 2017;7(6):1650–62.
[7] Yang T, Ke H, Wang Q, Tang Y, Deng Y, Yang H, et al. Bifunctional tellurium nanodots for photo-induced synergistic cancer therapy. ACS Nano 2017;11(10):10012–24.
[8] Younis MR, Wang C, An R, Wang S, Younis MA, Li ZQ, et al. Low power single laser activated synergistic cancer phototherapy using photosensitizer functionalized dual plasmonic photothermal nanoagents. ACS Nano 2019;13(2):2544–57.
[9] Jianliang S, Wei Z, Ruogu Q, Zong-Wan M, Haifa S. Engineering functional inorganic–organic hybrid systems: advances in siRNA therapeutics. Chem Soc Rev 2018;47(6):1969–95.
[10] Gang C, Yuna Q, Hang Z, Aftab U, Xiaojun H, Zaigang Z, et al. Advances in cancer theranostics using organic-inorganic hybrid nanotechnology. Appl Mater Today 2021;23:101003.
[11] Karousis N, Suarez-Martinez I, Ewels CP, Tagmatarchis N. Structure, properties, functionalization, and applications of carbon nanohorns. Chem Rev 2016;116(8):4850–83.
[12] He B, Shi Y, Liang Y, Yang A, Fan Z, Yuan L, et al. Single-walled carbon-nanohorns improve biocompatibility over nanotubes by triggering less protein-initiated pyroptosis and apoptosis in macrophages. Nat Commun 2018;9(1):2393.
[13] Zhang J, Sun Q, Bo J, Huang R, Zhang M, Xia Z, et al. Single-walled carbon nanohorn (SWNH) aggregates inhibited proliferation of human liver cell lines and promoted apoptosis, especially for hepatoma cell lines. Int J Nanomedicine 2014:9759–73.
[14] Murakami T, Ajima K, Miyawaki J, Yudasaka M, Iijima S, Shiba K. Drug-loaded carbon nanohorns: adsorption and release of dexamethasone *in vitro*. Mol Pharm 2004;1(6):399–405.
[15] Zhang M, Murakami T, Ajima K, Tsuchida K, Sandanayaka AS, Ito O, et al. Fabrication of ZnPc/protein nanohorns for double photodynamic and hyperthermic cancer phototherapy. Proc Natl Acad Sci USA 2008;105(39):14773–8.
[16] Dolmans DE, Fukumura D, Jain RK. Photodynamic therapy for cancer. Nat Rev Cancer 2003;3(5):380–7.
[17] Lo PC, Rodríguez-Morgade MS, Pandey RK, Ng DKP, Torres T, Dumoulin F. The unique features and promises of phthalocyanines as advanced photosensitisers for photodynamic therapy of cancer. Chem Soc Rev 2020;49(4):1041–56.
[18] Donzello MP, Viola E, Giustini M, Ercolani C, Monacelli F. Tetrakis(thiadiazole)porphyrazines. 8. Singlet oxygen production, fluorescence response and liposomal incorporation of tetrakis(thiadiazole)porphyrazine macrocycles [TTDPzM] (M = Mg(II)(H_2O), Zn(II), Al(III)Cl, Ga(III)Cl, Cd(II), Cu(II), 2H(I)). Dalton Trans 2012;41(20):6112–21.
[19] Pantò F, Adamo L, Giordano C, Licciardello C. Efficacy and safety of photodynamic therapy with RLP068 for diabetic foot ulcers: a review of the literature and clinical experience. Drugs Context 2020;9 2019–10-3.
[20] Jiang Z, Shao J, Yang T, Wang J, Jia L. Pharmaceutical development, composition and quantitative analysis of phthalocyanine as the photosensitizer for cancer photodynamic therapy. J Pharm Biomed Anal 2014:8798–804.
[21] Yang C, Wu T, Qi Y, Zhang Z. Recent advances in the application of vitamin E TPGS for drug delivery. Theranostics 2018;8(2):464–85.
[22] Zhang Z, Wang J, Chen C. Near-infrared light-mediated nanoplatforms for cancer thermo-chemotherapy and optical imaging. Adv Mater 2013;25(28):3869–80.
[23] Min Y, Roche KC, Tian S, Eblan MJ, McKinnon KP, Caster JM, et al. Antigen-capturing nanoparticles improve the abscopal effect and cancer immunotherapy. Nat Nanotechnol 2017;12(9):877–82.
[24] Wei X, Lin Q, Ning J, Qi Z, Lingxiao C, Xin J, et al. Metformin liposome-mediated PD-L1 downregulation for amplifying the photodynamic immunotherapy efficacy. ACS Appl Mater Inter 2021;13(7):8026–41.
[25] Ignacio M, Eduardo C, Maite A, Stephane C, Aurelien M. Intratumoural administration and tumour tissue targeting of cancer immunotherapies. Nat Rev Clin Oncol 2021:1–19.
[26] Urszula MC, Douglas PD, Jamie H, Kaye JW, Mark AT, Timothy MI. Immunomodulation by radiotherapy in tumour control and normal tissue toxicity. Nat Rev Immunol 2021. doi:10.1038/s41577-021-00568-1.